Supporting Information for

A ratiometric fluorescent probe for highly selective and sensitive detection of hypochlorite based on an oxidation of *N*-alkylpyridinium reaction

Lin Wang,[a] Lingliang Long,*[a] Liping Zhou,[a] Yanjun Wu,[a] Chi Zhang,[a] Zhixiang Han,[a] Junli Wang,[a] and Zulin Da[a]

[a] *Scientific Research Academy & School of Chemistry and Chemical Engineering, Jiangsu University, Zhenjiang, Jiangsu 212013 (P. R. China).*

Email: Longlingliang@163.com

Table of contents

Materials and instruments

Unless otherwise stated, all reagents were purchased from commercial suppliers and used without further purification. Solvents were purified and dried by standard methods prior to use. Twice-distilled water was used throughout all experiments. The solutions of various anions, cations, reactive oxygen species (ROS) and reactive nitrogen species (RNS) were prepared from NaF, KCl, KBr, NaI, $KClO_3$, $LiClO_4 \cdot 3H_2O$, Na_2CO_3, Na_2SO_4, $NaNO_3$, $NaNO_2$, KSCN, $NaBF_4$, CH_3COONa, $NaHSO_3$, $CuCl_2 \cdot 2H_2O$, $FeCl_3$, $Zn(NO_3)_2 \cdot 6H_2O$, $Pb(NO_3)_2$, $NiCl_2 \cdot 6H_2O$, 5.2% NaClO, 30% H_2O_2 respectively. $^1O_2$ was chemically generated from the H_2O_2/MoO_4^{2-} system in alkaline media.[1] Hydroxyl radical was generated by Fenton reaction.[2] Nitric oxide was generated from SNP (Sodium Nitroferricyanide (III) Dihydrate).[3] TLC analyses were performed on silica gel plates and column chromatography was conducted over silica gel (mesh 200-300), both of which were obtained from the Qingdao Ocean Chemicals. Melting points of compounds were measured on a Beijing Taike XT-4 microscopy melting point apparatus, and all melting points were uncorrected. Mass spectra were recorded on a LXQ Spectrometer (Thermo Scientific) operating on ESI. ^{1}H and ^{13}C-NMR spectra were recorded on a Bruker Avance 400 spectrometer operating at 400 MHz and 100 MHz respectively. Elemental (C, H, N) analysis were carried out using Flash EA 1112 analyzer. Electronic absorption spectra were obtained on a SHIMADZU UV-2450 spectrometer. Fluorescence spectra were measured on a Photon Technology International (PTI) Quantamaster fluorometer with 2 nm excitation and emission slit widths. The fluorescence images were acquired with a fluorescent microscope (Carl Zeiss, Axio Observer A1). The pH measurements were performed with a pH-3c digital pH-meter (Shanghai ShengCi Device Works, Shanghai, China) with a combined glass-calomel electrode.

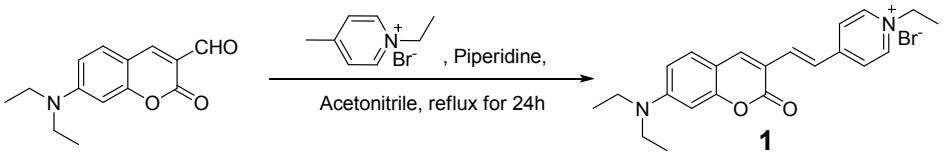

Synthesis of (E)-4-(2-(7-(diethylamino)-2-oxo-2H-chromen-3-yl)vinyl)-1-ethylpyridin-1-ium bromide (1)

One drop of piperidine was added to a solution of 7-diethylamino-coumarin- 3-aldehyde (506 mg, 2.06 mmol) and *N*-ethyl-4-methyl- pyridium bromide (500 mg, 2.47 mmol) in 20 mL acetonitrile. Then the mixture was heated to reflux for 24 h. After cooling to room temperature, solvent was removed under vacuum, and the resulting mixture was purified by column chromatography on silica gel (dichloromethane: methanol = 50: 1, v/v) to afford compound **1** as deep red solid (638.6 mg, 72.2%). Mp: 234-235 ^{o}C. ^{1}H NMR ($CDCl_3$, 400MHz), δ (ppm): 8.92 (d, J = 6.8 Hz, 2H), 8.22 (s, 1H), 8.09 (d, J =7.2 Hz, 2H), 7.81 (d, J =16 Hz, 1H), 7.73 (d, J =16 Hz, 1H), 7.44 (d, J =8.8 Hz, 1H), 6.61 (dd, J_1=8.8 Hz, J_2=2.4 Hz, 1H), 6.43 (d, J =2.4 Hz, 1H), 4.78 (q, J =7.2 Hz, 2H), 3.45 (q, J =7.2 Hz, 4H), 1.69 (t, J =7.2 Hz, 3H), 1.24 (t, J =7.2 Hz, 6H). ^{13}C NMR ($CDCl_3$, 100MHz), δ (ppm): 160.4, 156.8, 154.7, 152.4, 146.4, 143.2, 138.3, 130.9, 124.1, 122.5, 114.1, 109.9, 109.2, 96.8, 56.1, 45.2, 16.9, 12.6. MS (ESI) m/z 349.34 $[M+H]^+$. Elemental analysis calcd (%) for $C_{22}H_{25}BrN_2O_2$: C 61.54, H 5.87, N 6.52; found C 61.32, H 5.90, N 6.49.

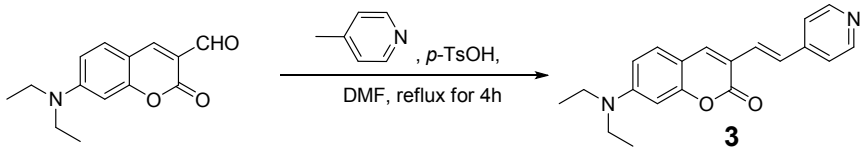

Synthesis of (E)-7-(diethylamino)-3-(2-(pyridin-4-yl)vinyl)-2H-chromen-2-one (3)

7-diethylaminocoumarin-3-aldehyde (800 mg, 3.26 mmol) and 4-methylpyridine (366 mg, 3.94 mmol) were added in 20 mL dry DMF, and then *p*-toluenesulfonic acid (1.55 g, 8.96 mmol) was added. After refluxed for 4 hours, the reaction mixture was poured into 100 ml of ice cold water and further stirred for 10 minutes. The precipitate was collected by filtration. The crude product was purified by chromatography on silica gel (dichloromethane: petroleum ether: ethanol = 20:40:1 for the first time; ethyl acetate: petroleum ether = 1:2 for the second time) to give the red solid compound **3** (436 mg, yield 41.8%). Mp: 163-164 ^{o}C. ^{1}H NMR (400 MHz, $CDCl_3$), δ (ppm): 8.54 (d, J = 6.4 Hz, 2H), 7.71 (s, 1H), 7.44 (d, J = 16.4 Hz, 1H), 7.35 (d, J = 6.4 Hz, 2H), 7.30 (d, J = 8.8 Hz, 1H), 7.22 (d, J = 16.4 Hz, 1H), 6.60 (dd, J_1 = 8.8 Hz, J_2 = 2.4 Hz, 1H), 6.50 (d, J = 2.4 Hz, 1H), 3.43 (q, J = 7.2 Hz, 4H), 1.23 (t, J = 7.2 Hz, 6H). ^{1}H NMR (100 MHz, $CDCl_3$), δ (ppm): 161.1, 156.0, 151.0, 150.1, 145.1, 140.4, 129.2, 127.9, 127.2, 120.8, 116.3, 109.3, 108.8, 97.1, 44.9, 12.5. MS (m/z): 321.4 $[M+H]^+$. Elemental analysis calcd (%) for $C_{20}H_{20}N_2O_2$: C 74.98, H 6.29, N 8.74; found C 74.69, H 6.32, N 8.70.

Procedure for fluorescence study

A stock solution of probe **1** was prepared at 2.5×10^{-4} M in THF, and a stock solution of various species (1×10^{-3} M) was prepared by dissolving an appropriate amount of species in water. Test solutions in 20 mM potassium phosphate buffer/THF (v/v 1: 3, pH 7.4) solution (5 mL) were prepared by placing 0.2 mL of probe **1** stock solution, 3.55 mL THF, and an appropriate aliquot of each testing species stock into a 5 mL volumetric flask, and then diluting the solution to 5 mL with 20 mM potassium phosphate buffer (pH 7.4). The resulting solution was shaken well and incubated at room temperature for 10 min before recording the spectra.

Determination of fluorescence quantum yield

Fluorescence quantum yield was determined using the solutions of quinine sulfate (Φ_F = 0.546 in 1N H_2SO_4)[4] as a standard. The quantum yield was calculated using the following equation:[5]

$$\Phi_{F(X)} = \Phi_{F(S)}\,(A_S F_X / A_X F_S)\,(n_X / n_S)^2$$

Where Φ_F is the fluorescence quantum yield, A is the absorbance at the excitation wavelength, F is the area under the corrected emission curve, and n is the refractive index of the solvents used. Subscripts S and X refer to the standard and to the unknown, respectively.

Determination of the detection limit

The detection limit was determined from fluorescence titration data based on a reported method.[6] According to the result of titration experiment, the graph of $(I_{min}-I) / (I_{min}-I_{max})$ versus log $[OCl^-]$ was plotted, where the I is the fluorescence intensity at 488 nm, I_{min} and I_{max} are the minimum and maximum fluorescence intensity at 488 nm respectively. A linear regression curve was then fitted (Fig. S4), and the intercept of the line at x-axis was taken as detection limit.

Kinetic Studies

The reaction rate constant of probe **1** with OCl^- was estimated under *pseudo*-first-order kinetic conditions (10 μM probe **1** and 150 μM OCl^-). The reaction of probe **1** with OCl^- in 20 mM potassium phosphate buffer/THF (v/v 1: 3, pH 7.4) was monitored by using the fluorescence intensity at 488 nm. The *pseudo*-first-order rate constant was determined by fitting the fluorescence intensities of probe **1** to the *pseudo*-first-order equation (1):[7]

$$\ln[(I_{max} - I_t) / I_{max}] = -k't \qquad (1)$$

where I_t and I_{max} are the fluorescence intensities at 488 nm at time t and the maximum value obtained after the reaction was completed. k' is the *pseudo*-first-order rate constant. Fig. S6 is the *pseudo*-first-order plot for the reaction of probe **1** with OCl^-. The negative slope of the line provides *pseudo*-first-order rate constant: k'.

Cell culture and fluorescence imaging

RAW264.7 cells were seeded in a 24-well plate in Dulbecco's modified Eagle's medium (DMEM) supplemented with 10% fetal bovine serum for 24 h. For evaluating the imaging ability of probe **1** to artificially loaded OCl^-, the cells were stained with probe **1** (1 μM) for 30 min at 37 °C. After washed with PBS buffer three times, the cells were further incubated with NaOCl (20 μM) for 30 min at 37 °C. Then the fluorescence images were acquired with a fluorescent microscope (Carl Zeiss, Axio Observer A1). For imaging endogenous OCl^- in Raw264.7 cells (endogenous generation of OCl^- was induced by the stimulant phorbol myristate acetate (PMA)[8]), the RAW264.7 cells were stained with probe **1** (1 μM) for 30 min at 37°C. After washed with PBS buffer three times, the cells were stimulated with PMA (2.5 μg mL^{-1}) for 2h at 37 °C. Then the cells were washed three times with PBS and used for fluorescence imaging. For the control experiment with MPO inhibitor, the RAW264.7 cells were stained with probe **1** (1 μM) for 30 min at 37 °C. After washed three times with PBS buffer, the cells were further incubated with 100 μM MPO inhibitor 4-aminobenzoic acid hydrazide (ABAH)[9] for 30 min at 37 °C and then stimulated with PMA (2.5 μg mL^{-1}) for 2h. After that, the cells were washed three times with PBS and used for fluorescence imaging.

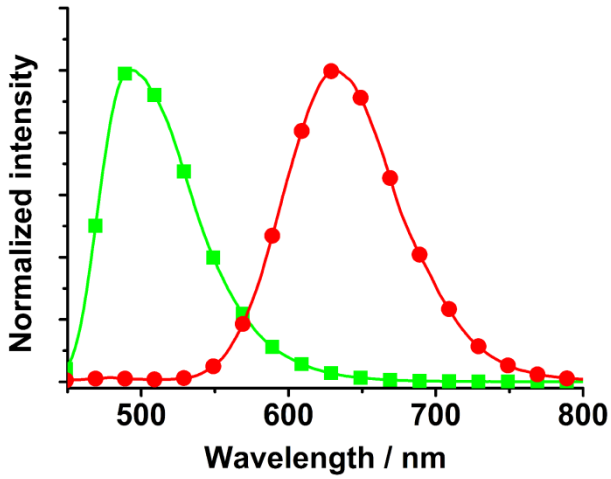

Figure S1. Normalized fluorescence emission spectra of probe **1** (●) and reference compound **3** (■) in 20 mM potassium phosphate buffer/THF (v/v 1: 3, pH 7.4), the excitation wavelength was at 420 nm.

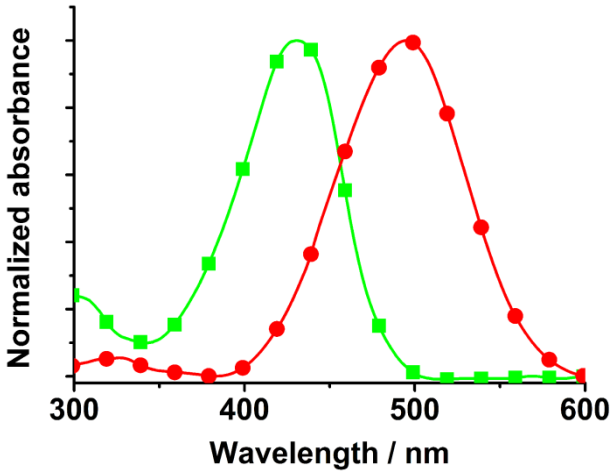

Figure S2. Normalized absorption spectra of probe **1** (●) and reference compound **3** (■) in 20 mM potassium phosphate buffer/THF (v/v 1: 3, pH 7.4).

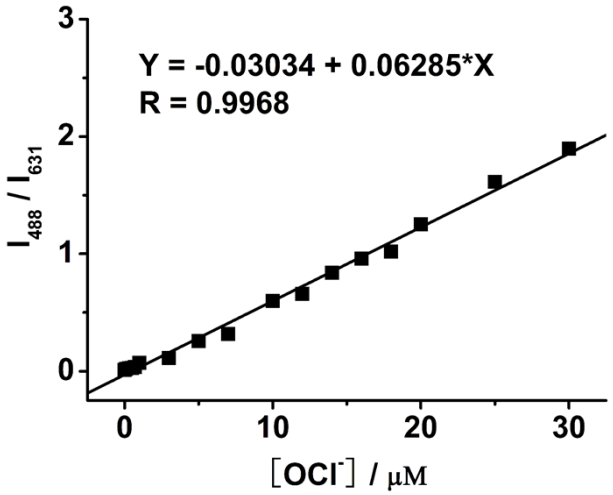

Figure S3. The emission ratio (I_{488}/I_{631}) of probe **1** (10 μM) to various amount of OCl^- (0 μM to 30 μM). The data were acquired after incubation of probe **1** with OCl^- for 10 min at room temperature. Excitation was performed at 420 nm.

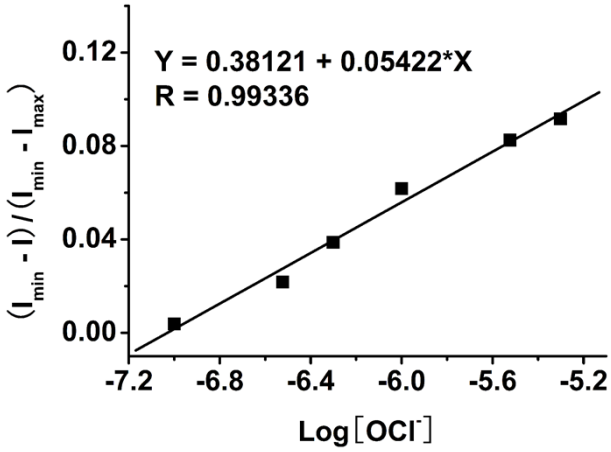

Figure S4. Plot of (I_{min}- I) / (I_{min}-I_{max}) versus log [OCl^-] for probe **1**. Calculated detection limit = 0.093 μM.

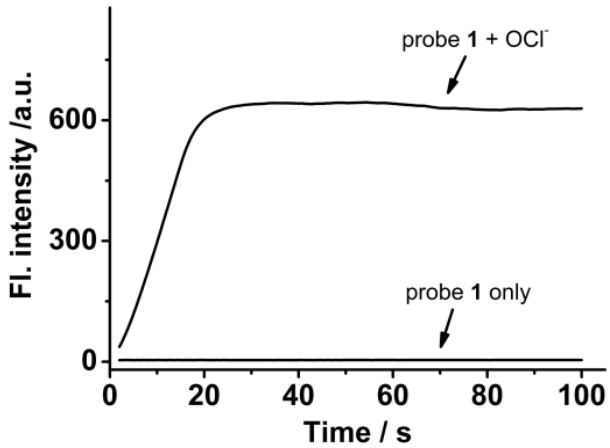

Figure S5. Time dependent fluorescence intensity (488 nm) changes of probe **1** (10 μM) in the absence or presence of OCl^- (150 μM) in 20 mM potassium phosphate buffer/THF (v/v 1: 3, pH 7.4).

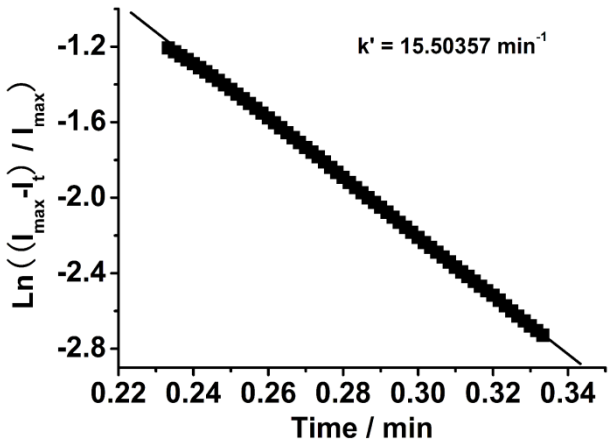

Figure S6. *Pseudo*-first-order kinetic plot of the reaction of probe **1** (10 μM) incubated with OCl^- (150 μM) in 20 mM potassium phosphate buffer/THF (v/v 1: 3, pH 7.4). Slope= -15.50357 min^{-1}.

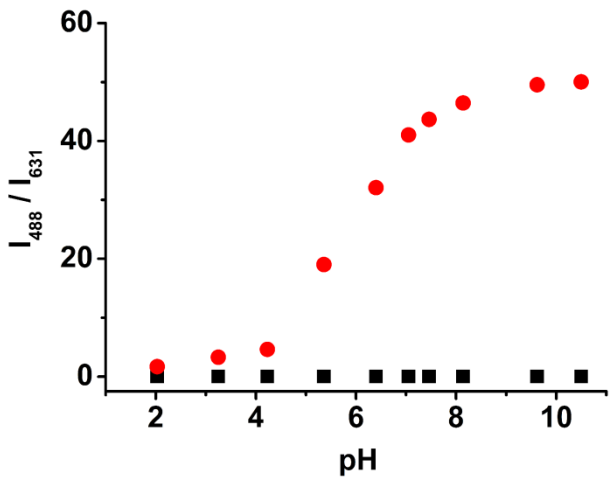

Figure S7. The variations of emission ratio (I_{488} / I_{631}) of probe **1** (10 μM) in the absence (■) or presence (●) of OCl^- (90 μM) as a function of pH. Excitation wavelength was 420 nm.

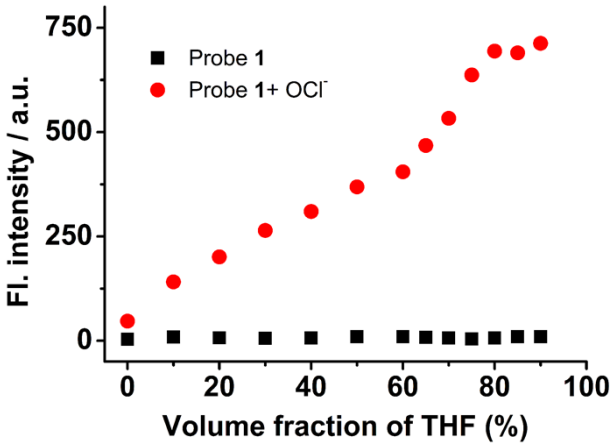

Figure S8. The effect of THF volume fraction on fluorescence response of probe **1** (10 μM) to OCl^- (90 μM). Excitation was provided at 420 nm, and the fluorescence intensity at 488 nm was measured.

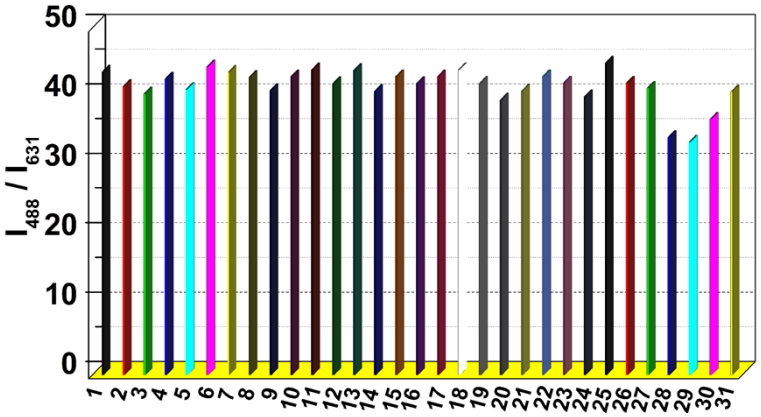

Figure S9. Ratiometric fluorescent response of probe **1** (10 μM) to OCl^- (90 μM) in the presence of other species (90 μM). 1) blank; 2) H_2O_2; 3) ·OH; 4) $^1O_2$; 5) NO·; 6) F^-; 7) Cl^-; 8) Br^-; 9) I^-; 10) ClO_3^-; 11) ClO_4^-; 12) CO_3^{2-}; 13) SO_4^{2-}; 14) NO_3^-; 15) NO_2^-; 16) SCN^-; 17) BF_4^-; 18) CH_3COO^-; 19) HSO_3^-; 20) Cu^{2+}; 21) Fe^{3+}; 22) Zn^{2+}; 23) Pb^{2+}; 24) Ni^{2+}; 25) Gly; 26) Val; 27) Phe; 28) Ala; 29) Leu; 30) Lys; 31) Glucose. The excitation wavelength was 420 nm.

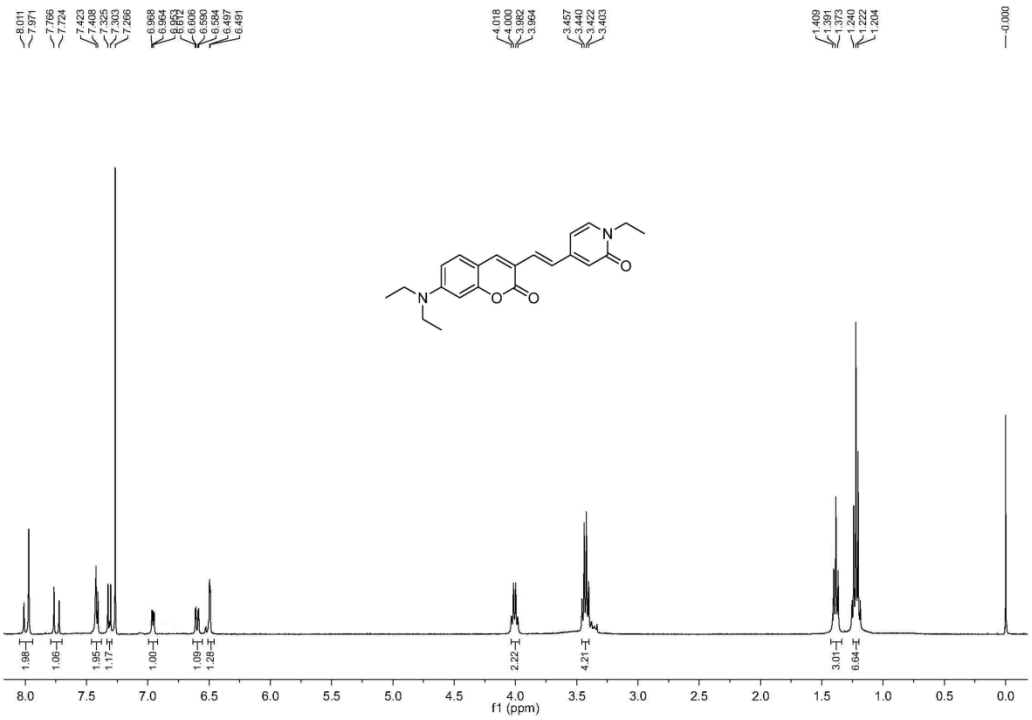

Figure S10. ^{1}H NMR spectra of the isolated product of probe **1** + NaOCl.

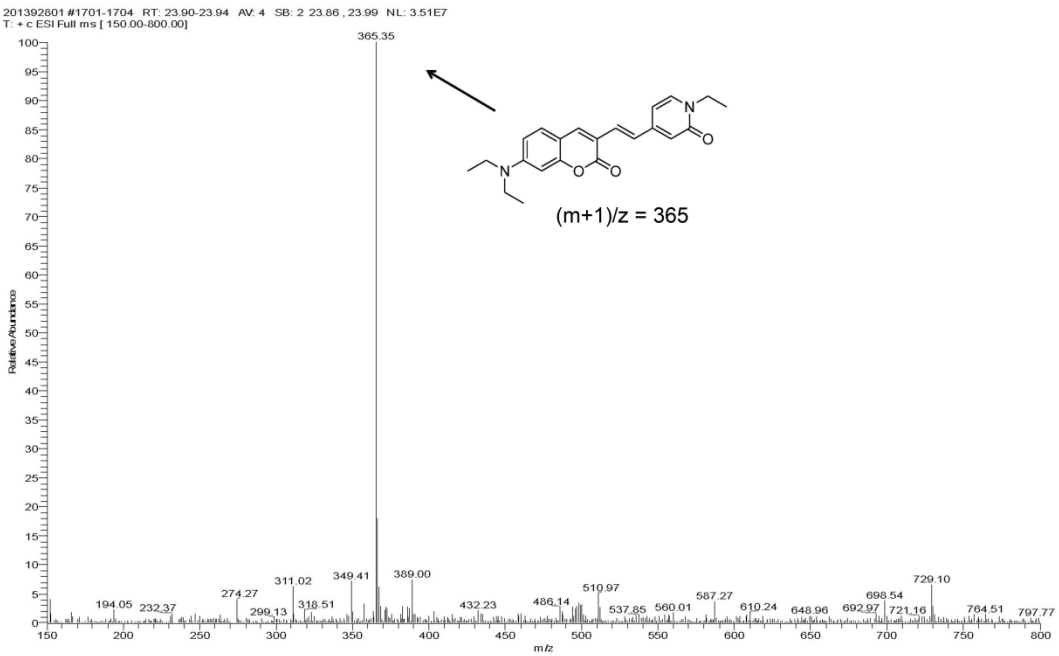

Figure S11. The ESI-Ms spectra of the isolated product of probe **1** + NaOCl.

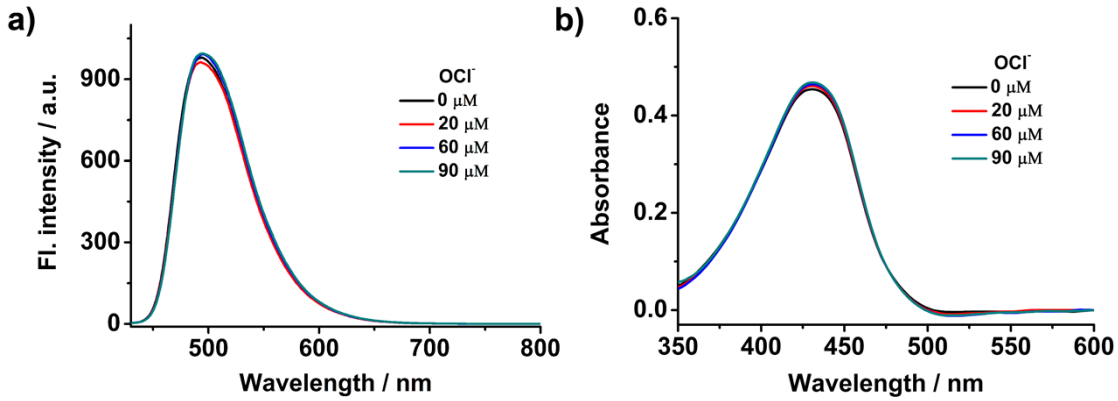

Figure S12. Fluorescence emission spectra (a) and absorption spectra (b) of reference compound **3** (10 μM) in 20 mM potassium phosphate buffer/THF (v/v 1: 3, pH 7.4) with various concentration of OCl^-.

Computational details

The ground state structures of the probe were optimized using density functional theory (DFT) with B3LYP functional and 6-31+G** basis set. The vertical excitation energies were carried out with the time dependent DFT (TD-DFT), based on the optimized structure of the ground state. All these calculations were performed with Gaussian 09 program.

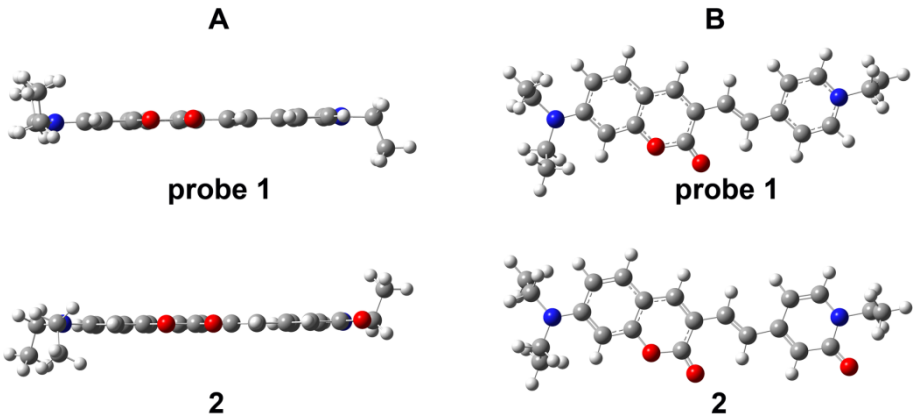

Figure S13. Optimized ground-state geometries of the probe **1** and compound **2**. A) The side-view; B) the top-view.

Table S1. Selected electronic excitation energies (eV), oscillator strengths (f), main configurations, and CI coefficients of the low-lying excited states of the probe **1** and compound **2**. The data were calculated by TDDFT//B3LYP/6-31G** based on the optimized ground state geometries.

compound	Electronic Transition	TDDFT//B3LYP/6-31G**			
		Excitation Energy[a]	f[b]	Composition[c]	CI[d]
1	$S_0 \rightarrow S_1$	2.38 eV (520 nm)	1.5152	H→L	0.70728
	$S_0 \rightarrow S_2$	3.34 eV (371 nm)	0.2188	H→L+1	0.59824
	$S_0 \rightarrow S_5$	3.76 eV (329 nm)	0.1439	H-2→L	0.48737
2	$S_0 \rightarrow S_1$	2.86 eV (433 nm)	1.5547	H→L	0.70367
	$S_0 \rightarrow S_9$	4.51 eV (275 nm)	0.1084	H→L+3	0.64429
	$S_0 \rightarrow S_{15}$	5.12 eV (242 nm)	0.255	H-3→L+1	0.60134
	$S_0 \rightarrow S_{20}$	5.28 eV (235 nm)	0.1079	H-1→L+3	0.47798

[a] Only selected excited states were considered. The numbers in parentheses are the excitation energy in wavelength. [b] Oscillator strengths. [c] H stands for HOMO and L stands for LUMO. [d] The CI coefficients are in absolute values.

Application of probe 1 in real water sample analysis

The crude water samples from Yangtzi River, pond water and tap water were firstly filtered through microfiltration membrane. And then, the pH value of the water samples was adjusted to 7.4 by addition of aliquot aqueous sodium hydroxide. For determination of OCl^- in water samples, 1.25 mL of water sample was added to 3.75 mL of probe **1** (13.33 μM) in THF. The resulting solution was shaken well and incubated for 10 min at room temperature. After that, the emission ratio (I_{488}/I_{631}) was recorded. The OCl^- in Yangtzi River and pond water were not detected, and the concentration of OCl^- in tap water was quantified to be 8.65 ± 0.08 μM. Next, the Yangtzi River sample and pond water sample were spiked with standard OCl^- solutions at different concentration levels and then analyzed with probe **1**, the results are shown in Table S2.

Table S2. Determination of OCl^- concentrations in natural water samples.

Sample	OCl^- spiked (mol L^{-1})	OCl^- recovered (mol L^{-1}) [a]	Recovery (%)
Yangtzi River 1	0	Not detected	-
Yangtzi River 2	2.00×10^{-5}	$(1.96 \pm 0.05) \times 10^{-5}$	98.0
Yangtzi River 3	1.00×10^{-4}	$(0.94 \pm 0.08) \times 10^{-4}$	94.0
Pond water 1	0	Not detected	-
Pond water 2	2.00×10^{-5}	$(1.98 \pm 0.03) \times 10^{-5}$	99.0
Pond water 3	1.00×10^{-4}	$(1.03 \pm 0.04) \times 10^{-4}$	103.0

[a] Relative standard deviations were calculated based on three times of measurement.

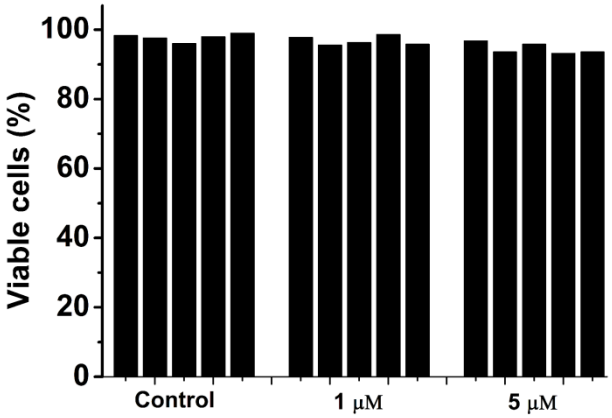

Figure S14. Cytotoxicity of probe **1** in cultured RAW264.7 macrophage cells. The cells were incubated with the probe at 1 and 5 μM of probe **1** for 24 h (n = 5). The cell viability was measured by the MTT assay, and the data are reported as the percentage relative to the untreated cells.

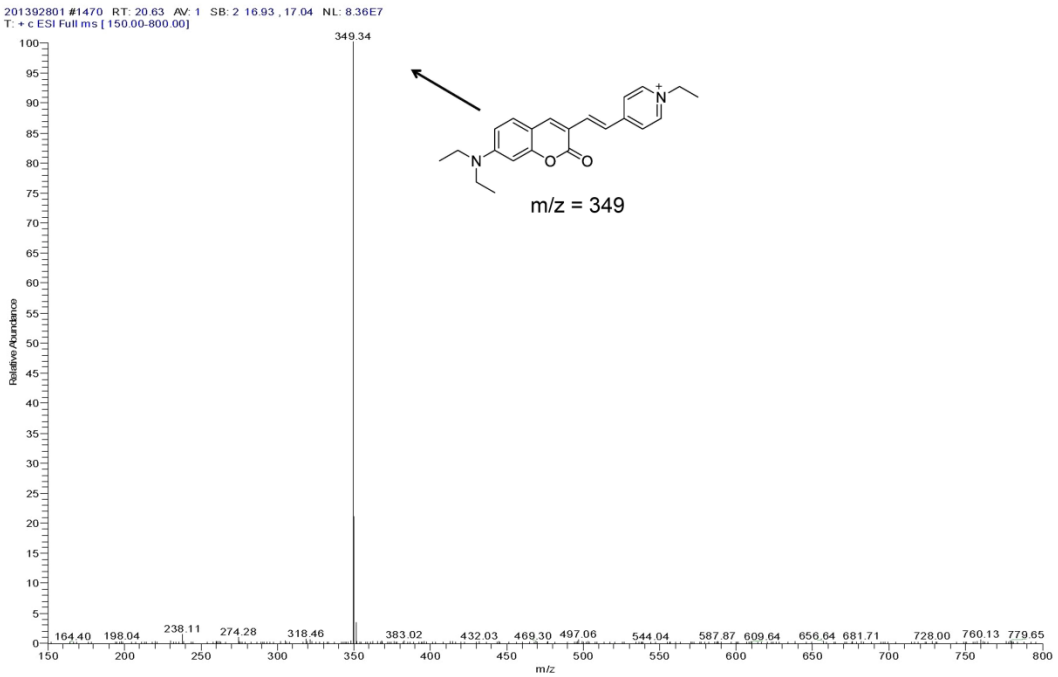

Figure S15. ESI-Ms spectra of probe **1**.

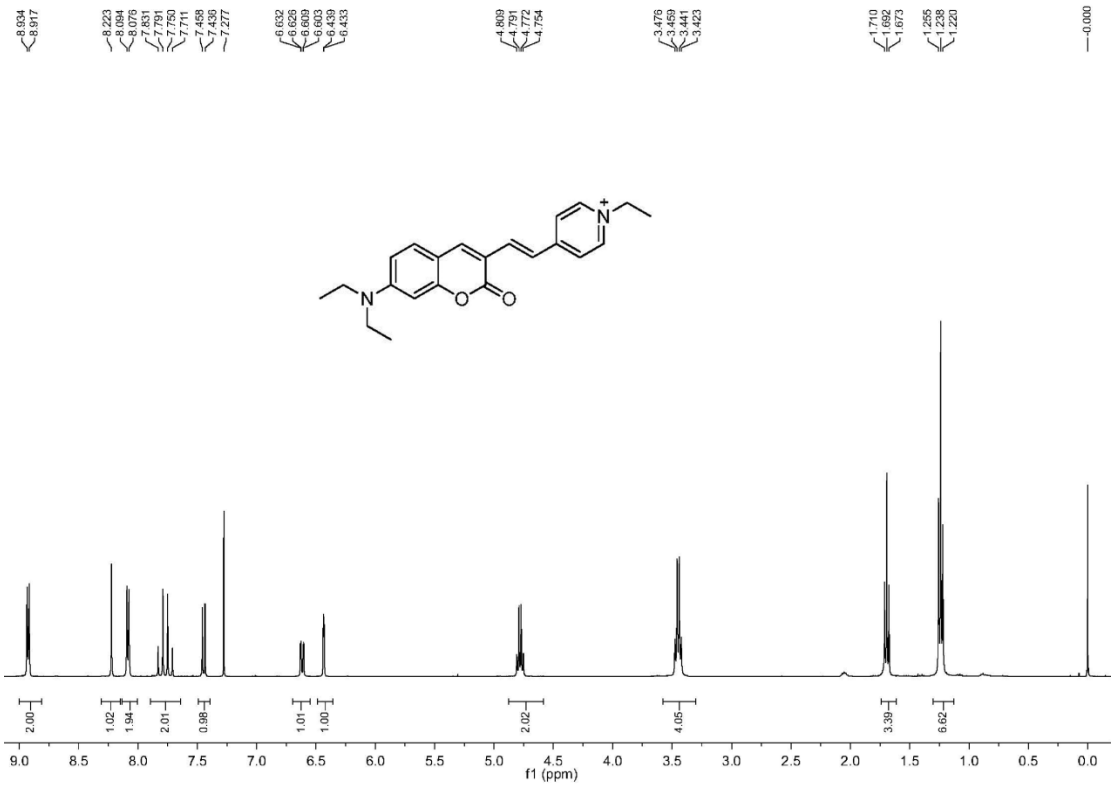

Figure S16. ^{1}H NMR spectra of probe **1**.

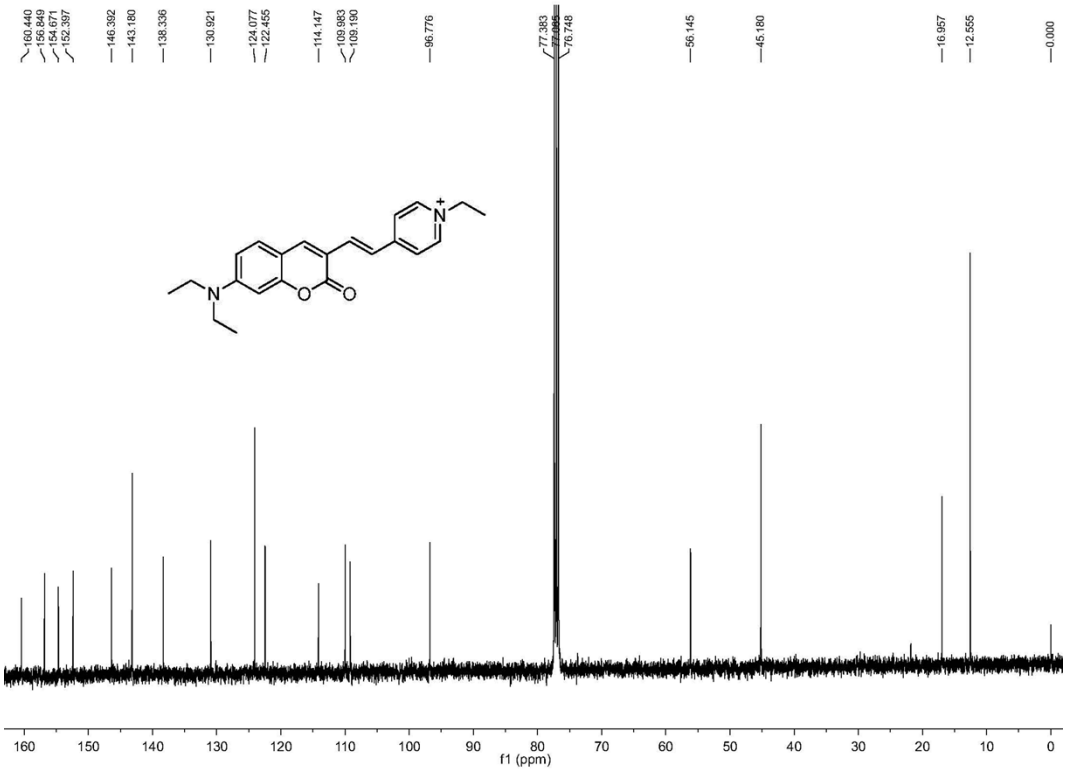

Figure S17. ^{13}C NMR spectra of probe **1**.

References

1 (a) J. M. Aubry, *J. Org. Chem.,* 1989, **54**, 726-728; (b) N. Umezawa, K. Tanaka, Y. Urano, K. Kikuchi, T. Higuchi, T. Nagano, *Angew. Chem. Int. Ed.,* 1999, **38**, 2899-2901.

2 (a) H. H. Fenton, *Chem. News,* 1876, **33**, 190-190; (b) K. Setsukinai, Y. Urano, K. Kakinuma, H. J. Majima, T. Nagano, *J. Biol. Chem.,* 2003, **278**, 3170-3175.

3 (a) Z. Sun, F. Liu, Y. Chen, P. K. H. Tam, D. Yang, *Org. Lett.,* 2008, **10**, 2171-2174; (b) Y. Yang, H. J. Cho, J. Lee, I. Shin, J. Tae, *Org. Lett.,* 2009, **11**, 859-861.

4 J. N. Demas, G. A. Crosby, *J. Phys. Chem.*, 1971, **75**, 991-1024.

5 (a) C. A. Parker, W. T. Rees, *Analyst*, 1960, **85**, 587-600; (b) S. F. Forgues, D. Lavabre, *J. Chem. Educ.*, 1999, **76**, 1260-1264; (c) A. Ajayaghosh, P. Carol, S. Sreejith, *J. Am. Chem. Soc.*, 2005, **127**, 14962-14963.

6 (a) M. Shortreed, R. Kopelman, M. Kuhn, B. Hoyland, *Anal. Chem.*, 1996, **68**, 1414-1418; (b) A. Caballero, R. Martínez, V. Lloveras, I. Ratera, J. Vidal-Gancedo, K. Wurst, A. Tarraga, P. Molina, J. Veciana, *J. Am. Chem. Soc.*, 2005, **127**, 15666-15667; (c) W. Lin, L. Long, W. Tan, *Chem. Commun.*, 2010, **46**, 1503-1505; (d) W. Chen, W. Gong, Z. Ye, Y. Lin, G. Ning, *Dalton Trans.*, 2013, **42**, 10093-10096; (e) B. Chandra, S. P. Mahanta, N. N. Pati, S. Baskaran, R. K. Kanaparthi, C. Sivasankar, P. K. Panda, *Org. Lett.*, 2013, **15**, 306-309.

7 (a) Y. Lin, Y. Pen, W. Su, K. Liau, Y. Wen, C. Tu, C. Sun, and T. J. Chow, *Chem. Asian J.*, 2012, **7**, 2864-2871; (b) T. J. Dale, J. J. Rebek, *J. Am. Chem. Soc.*, 2006, **128**, 4500-4501.

8 (a) S. Liu, S. Wu, *Org. Lett.,* 2013, **15**, 878-881; (b) M. Wolfson, L. C. McPhail, V. N. Nasrallah, R. Snyderman, *J. Immunol.,* 1985, **135**, 2057-2062.

9 S. Kumar, S. Patel, A. Jyoti, R. Keshari, A. Verma, M. Barthwal, M. Dikshit, *Cytometry, Part A,* 2010, **77**, 1038-1048.